JOURNAL OF PROPULSION AND POWER
Vol. 10, No. 2, March–April 1994

Feasibility Study of a Contained Pulsed Nuclear Propulsion Engine

Alexander G. Parlos*
Texas A&M University, College Station, Texas 77483
and
John D. Metzger†
Grumman Aerospace & Electronics, Bethpage, New York 11714

The result of a feasibility analysis of a contained pulsed nuclear propulsion (CPNP) engine concept utilizing the enormously dense energy generated by small nuclear detonations is presented in this article. This concept was initially proposed and studied in the 1950s and 1960s under the program name HELIOS. The current feasibility of the concept is based upon material technology that has advanced to a state that allows the design of pressure vessels required to contain the blast associated with small nuclear detonations. The impulsive nature of the energy source provides the means for circumventing the material thermal barriers that are inherent in steady-state nuclear propulsion concepts. The rapid energy transfer to the propellant results in high thrust levels for times less than 1 s following the detonation. The preliminary feasibility analysis using off-the-shelf material technology appears to indicate that the CPNP concept can have thrust-to-weight ratios on the order of 1 or greater. Though the specific impulse is not a good indicator for impulsive engines, an operating-cycle-averaged specific impulse of approximately 1000 or greater seconds has been calculated.

Nomenclature

E = Young's modulus
$F_N(t)$ = thrust from supersonic nozzle, Eq. (31)
f_p = fraction of the peak pressure—shape factor, Eq. (14)
g = acceleration of gravity, Eq. (11)
H_l = sensible and latent heat necessary to vaporize liner, Eqs. (22) and (33)
$I_{sp}(t)$ = specific impulse, Eq. (32)
k_l = thermal conductivity of liner material, Eq. (33)
M_{veh} = mass of the vehicle, Eq. (34)
$M(W)$ = mass (weight) of containment vessel, Eq. (10)
m, m_0, m_d, m_v = total mass, mass of propellant, mass of nuclear device, and mass of vaporized liner, Eq. (18)
$\dot{m}(t)$, $\dot{m}(t)_{sonic}$ = mass flow rate, Eq. (28), and sonic mass flow rate, Eq. (27)
n = number of nuclear detonations, Eq. (34)
p^*, t^* = final pressure and time to reach final pressure, Eq. (4)
$\hat{p}$, $\hat{t}$ = peak pressure and time of duration, Eq. (4)
$p_{ambient}$ = ambient pressure at nozzle outlet, Eq. (23)
$p_{cont}(t)$ = time-dependent pressure in the containment vessel, Eq. (24)
$p(t)$ = internal pressure load, Eq. (4)
p_w = pressure at the vessel wall, Eq. (13)
p_0 = equilibrium pressure, Eq. (4)
R = vessel radius
T = period, Eq. (3)
$T_{cont}(t)$ = time-dependent temperature in the containment vessel, Eq. (25)
T_i = initial temperature of liner material, Eq. (33)
t_{exh} = time to exhaust vessel, Eqs. (27) and (29)
$u(t)$, u_{max} = vessel wall displacement, Eqs. (1) and (5), and maximum vessel wall displacement, Eq. (7)
$V_e(t)$ = exit velocity from supersonic nozzle, Eq. (30)
V_{vessel} = containment vessel volume
Y = yield of nuclear device in tons of energy
α_l = thermal diffusivity of liner material, Eq. (33)
γ, γ_0, γ_d, γ_v = ratio of the specific heats: propellant-vapor mixture, propellant, device, vaporized liner
Δh = thickness vessel
ε_{max} = maximum strain, Eq. (8)
μ = metric tonnes of the vessel per ton of yield, Eq. (11)
ν = Poisson's ratio
$\rho_{cont}(t)$ = time-dependent density of the propellant-vapor mixture in the containment vessel
ρ_s, ρ, ρ_l = vessel material density, initial density of the propellant-vapor mixture, density of liner material
σ_{max} = maximum stress, Eq. (8)
ω = natural frequency, Eq. (2)

Introduction

EVEN though the use of nuclear explosives appears to have been limited to destructive purposes, it appears feasible to use this extraordinary energy source for peaceful purposes. There are fundamental and compelling reasons for the utilization of nuclear explosives for space propulsion. First, there is no known energy source that is more compact than the one provided by nuclear explosives. Very high propellant velocities can be achieved as a result of the enormous amount of energy produced per unit mass of a nuclear explosive. The

Received Nov. 4, 1992; revision received May 10, 1993; accepted for publication June 21, 1993.
*Associate Professor, Department of Nuclear Engineering.
†Engineering Specialist, Nuclear Advanced Technology, M/S B09-25.

second, and more important, reason for using nuclear explosives is that the impulsive nature of the energy source provides a means for circumventing the thermal barriers inherent in steady-state nuclear propulsion systems.

Almost all nuclear thermal propulsion (NTP) systems currently under consideration are limited in performance by the allowable temperatures in the engine structure. Considering other factors constant, engine performance, or the I_{sp}, increases as the square root of the propellant temperature in the rocket chamber. Solid-core NTP concepts contain fuel elements which must remain structurally intact at temperatures that are much higher than the maximum propellant temperature in the thrust chamber. This means that the mixed-mean propellant temperature in solid-core NTP concepts will be limited to approximately 3000 K.

Gas-core NTP concepts attempt to circumvent the material temperature limitations of the solid nuclear fuel elements by using a less dense, high-temperature fissioning gas as the energy source, which heats the hydrogen propellant through radiation. This fundamental approach is also the underlying principle of fusion and antiproton propulsion concepts. The limiting material consideration of a gas-core engine is the temperature limitation of the chamber containing the fissioning-gas. If the fundamental issues related to plasma containment are resolved, considerable improvements in exhaust temperatures, when compared to solid-core NTP concepts, can be achieved by using gas-core NTP systems.[1,2]

CPNP concepts attempt a different approach in circumventing the materials limitations, and yet obtain high chamber temperatures. Preliminary calculations indicate that by reducing the engine operating time, the duration of interaction between the propellant and the engine structure to several milliseconds, significant momentum can be transferred and the thermal waves will not have time to penetrate the vessel structure. Experiments have confirmed that common materials such as aluminum or steel can withstand surface temperatures of over 80,000 K for short time periods with only nominal surface ablation.[3]

Interest in utilizing nuclear explosives as the energy source of high-performance space engines dates back to the early 1950s.[3] In the late 1950s this interest was intensified, resulting in the initiation of a number of analytical and experimental studies to address the basic physical and engineering issues of the concept. In the U.S. two pulsed nuclear propulsion concepts were investigated during the 1950s and 1960s.[3] The concept which appears to have received most of the attention and resources was the unconfined pulsed nuclear propulsion, equivalent to an external combustion engine. In this concept the impulsive energy generated from the nuclear explosion is external to the vehicle, and it is used to propel a spacecraft via pusher-plates. In the literature this concept has been referred to as ORION.[3] Recently, alternate versions of ORION have been reported by Augenstein.[4]

The other impulsive concept found in the early literature is a CPNP system. In the literature this was referred to as the HELIOS concept, and even though it has been recognized and discussed in a number of citations, its originator is unknown.[5,6] From the results of the HELIOS concept studies found in the open literature, the following conclusions are made:

1) There are a number of engineering design issues that must be addressed before a definite positive statement can be made at about the HELIOS concept. However, in view of the significant progress made in material science and engineering, and in computational hydrodynamic and structural analysis capabilities since the last serious analysis of this concept, there is no apparent reason to doubt that such efforts would result in a working engine.[7]

2) The practicality of this concept will critically depend on the availability of a suitable nuclear charge, especially with respect to reliability. Achievement of a low charge mass is of great importance. The use of transuranic materials, such as Am^{242m}, for the nuclear charge appears to result in significant mass savings.

A number of initial feasibility studies of this concept had been performed in the early to mid 1960s.[5,7] Significant effort had been invested into system studies seeking, for stated missions, the engine configuration and operating parameters which give minimum initial weight and number of pulses. A number of analytical studies had been performed on technical problems most relevant to this concept. The main areas of concentration had been the explosion hydrodynamics, heat transfer to the vessel wall, pulsed propellant discharge behavior, nozzle design, and engine-vehicle coupling. Additionally, experimental studies of layered structural materials for potential use in the pressure vessel walls were performed. More recently, a review article summarizing a number of experiments demonstrating pulsed detonation concepts, and the relevant numerical simulations appeared in the literature.[8]

The primary feasibility study for a CPNP engine presented here addresses the containment of a nuclear detonation in a monolithic spherical vessel with a metal liner. The outcome of this analysis will be used to investigate the propulsive performance of a CPNP system. The analytical and hydrodynamic analysis presented for the containment of a nuclear detonation in a monolithic spherical vessel with a metal liner was performed at Los Alamos National Laboratory for another application.[9] The results of the Los Alamos study provided the incentive to investigate the application of contained nuclear detonations to a propulsion system.

In view of the apparent technology readiness level of the HELIOS concept components, it is believed that a feasible engine with attractive performance characteristics can be designed and tested for possible use in planned manned and/or cargo missions required to accomplish the Space Exploration Initiative (SEI). This article will present the results of work characterizing the containment of a nuclear detonation in a spherical pressure vessel, the results of a literature search of current material technology, and the results of a CPNP system performance analysis. This article does not address specific engineering design issues that are necessary for a conceptual design of a CPNP system.

CPNP Engine Analysis

As previously mentioned, there have been two distinct variations of pulsed nuclear propulsion engines which have been studied in some detail. The CPNP approach, HELIOS, provides an almost complete containment of the explosive by means of a strong pressure vessel which absorbs the initial shock wave and then expands the explosion debris and the gas initially in the vessel through a conventional supersonic nozzle. The charge residues and the hydrogen propellant are brought to a high temperature by the explosion, ranging from several thousands to several tens of thousands of degrees Kelvin. Essentially, all of the explosion products are employed as propellant, and the system's performance is limited primarily by the maximum impulsive chamber pressure and temperature which can be tolerated by the designed pressure vessel. The cycle is repeated up to several thousand times, depending upon the specific ΔV requirements of the mission under consideration and the yield of the explosive used, at intervals on the order of 1–10 s or longer. Depending upon the cargo, the high impulsive acceleration loads are moderated by a system of shock absorbers between the engine and the vehicle. A simple schematic diagram of the contained pulsed nuclear propulsion concept is depicted in Fig. 1.

The CPNP concept is inherently unsteady, and therefore, determination of the time scales of interest is of utmost importance. In general, two time regimes are defined, with only the first one being of interest in this analysis: the time directly following the nuclear detonation to approximately 0.01 s, and

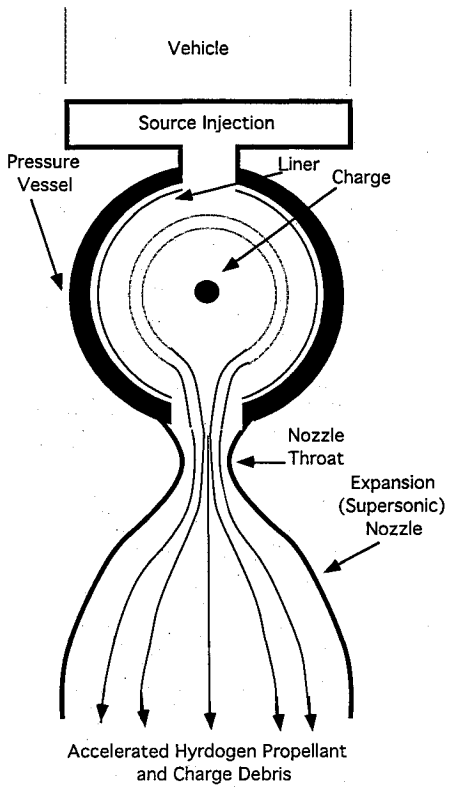

Fig. 1 Schematic diagram of the contained pulsed CPNP nuclear propulsion concept.

the time between 0.01 and 1–10 s. The early time regime, investigated in this analysis, is characterized by the initial radiation loading of the containment wall followed by the expansion of the debris, the compression of the propellant, the subsequent pressure shocking of the vessel wall, and the deflection of the vessel. In this time regime, the structural response of the vessel and the thermal response of the hydrogen propellant can be studied using a one-dimensional radiation-coupled hydrodynamic computer program. The latter time regime is characterized by the damping of the gas motion in the vessel and the establishment of thermal conduction and advection energy transfer between the gases in the vessel and the vessel wall.[9]

In the results presented of the analysis, only the initial time regime is investigated by scaling the vessel based on a simplified analytic approach. This analytical approach is found to be accurate when compared to a more detailed analyses using the one-dimensional, radiation-couple hydrodynamics code CHARTD.[9,10] The propellant mass flow rate transient through the nozzle sonic throat is evaluated using the solution to the unsteady energy conservation equation in the vessel. The expansion of the hydrogen propellant through a supersonic nozzle is investigated using a quasisteady approach, enabling the calculation of the engine thrust and specific impulse. The initial conditions for the temperature transients are obtained from the results of the one-dimensional, radiation-coupled hydrodynamic computer program CHARTD.[9]

For the purposes of this preliminary analysis, it assumed that the nuclear device was completely vaporized and no solid debris impinged upon the vessel wall. The analysis did not consider radiation effects, either primary or secondary. The analysis also assumed that as a result of the rapid and effective energy transfer to the hydrogen propellant and its subsequent rapid blowdown, no significant amount of energy is deposited on the vessel wall, and thus, we have not done a thermal analysis of the vessel walls. This is an approximation, and its validity needs to be investigated in further analysis. We suggest that the latter time regime can be investigated in some detail by using a one-dimensional thermal computer program that models the melting and the vaporization of the vessel wall, and the ensuing condensation of the vaporized material.

Pressure Vessel Scaling

A monolithic, spherical steel vessel with a large aspect ratio containing a blast responds like a thin elastic shell; i.e., it acts as a driven, undamped oscillator. The displacement of the shell $u(t)$ for an internal pressure load $p(t)$ is given by[9]

$$\ddot{u}(t) + \omega^2 u(t) = \frac{p(t)}{\rho_s \Delta h} \tag{1}$$

with the natural frequency defined by

$$\omega = \sqrt{\frac{2E}{\rho_s R^2 (1 - \nu)}} \tag{2}$$

T of the vessel response is given by

$$T = (2\pi/\omega) \tag{3}$$

To obtain a solution to Eq. (1), a pressure load shape must be assumed. A pressure load shape characteristic of a nuclear detonation in an initially low-pressure vessel can be expressed as

$$p(t) = \begin{cases} \hat{p},\ 0 < t < \hat{t} \\ \left(\dfrac{p^* - p_0}{t^* - \hat{t}}\right)(t - \hat{t}) + p_0,\ \hat{t} < t < t^* \\ p^*,\ t > t^* \end{cases} \tag{4}$$

This is a square leading pressure spike with an amplitude of $\hat{p}$, followed by a ramp from p_0 to some pressure p^* associated with the increase in mass in the vessel due to liner vaporization.

Simplifying the pressure load profile by neglecting the ramp, that is assuming that $p_0 = p^*$, and using the pressure load shape to solve Eq. (1), results in the following conservative expression for the general displacement of the vessel walls[9]:

$$u(t) = \begin{cases} \dfrac{\hat{p}}{\omega^2 \rho_s \Delta h}[1 - \cos(\omega t)],\ t < \hat{t} \\ \dfrac{p_0}{\omega^2 \rho_s \Delta h}\{(\delta - \omega\hat{t})\sin(\omega t) + [1 - \cos(\omega t)]\},\ t > \hat{t} \end{cases} \tag{5}$$

where

$$\delta = (\hat{p}\hat{t}\omega/p_0) \tag{6}$$

In view of Eq. (5), the maximum vessel wall displacement is given by

$$u_{\max} = \frac{p_0}{\omega^2 \rho_s \Delta h}\left[1 + \sqrt{1 + \delta^2\left(1 - \frac{p_0}{\hat{p}}\right)^2}\right] \tag{7}$$

$\varepsilon_{\max}$ in the elastic region of the vessel wall material can be expressed in terms of $\sigma_{\max}$ using Hook's Law:

$$\varepsilon_{\max} = \frac{u_{\max}}{R} = \frac{\sigma_{\max}(1 - \nu)}{E} \tag{8}$$

Assuming that the gamma-gas law applies,[11] the equilibrium pressure in the vessel is expressed as

$$p_0 = \frac{(\gamma - 1)Y}{V_{\text{vessel}}} = \frac{(\gamma - 1)Y}{\frac{4}{3}\pi R^3} \tag{9}$$

where V_{vessel} is the volume of a sphere with R, γ is the ratio of the specific heat for the vaporized device and the propellant gas mixture, and Y is the total deposited yield energy of the device. The weight of the shell is calculated as

$$W = Mg = (4\pi R^2 \Delta h \rho_s) g \tag{10}$$

where M is the mass of the shell and the constant g is the acceleration of gravity, 9.8 m/s^2.

The variable μ defines the vessel's effectiveness in containing the blast. It is defined as the ratio of the vessel mass divided by the yield energy; i.e., metric tonnes of vessel mass per ton (4.2×10^9 J) of nuclear yield energy. From Eq. (2) and Eqs. (7–10), μ is determined to be[9]

$$\mu = \frac{M}{Y} = \frac{3(\gamma - 1)\rho_s}{2\sigma_{max}} \left[1 + \sqrt{1 + \delta^2 \left(1 - \frac{p_0}{\hat{p}} \right)^2} \right] \tag{11}$$

The quantity δ is related to the impulse delivered to the shell, and assuming a strong shock this quantity can be expressed as[9]

$$\delta = \frac{1}{3(\gamma - 1)} \sqrt{\frac{2Em}{\rho_s (1 - \nu) Y}} \tag{12}$$

where m is the total mass impacting the shell wall. Following the reflection of the pressure shock from a rigid wall, the ratio of p_0 behind the shock to p_w is given by[9,11]

$$\frac{p_0}{p_w} = \frac{(\gamma - 1)}{(3\gamma - 1)} \tag{13}$$

The square wave approximation, Eq. (4), to the leading pressure spike can be expressed as

$$\hat{p} \approx f_p p_w \tag{14}$$

The value of f_p approaches 1.0 for vessels with a small radius and low initial fill pressures, and it approaches 0 for large vessels and high initial fill pressures.[9] Substituting Eqs. (12–14) into Eq. (11) results in

$$\mu = \frac{3(\gamma - 1)\rho_s}{2\sigma_{max}} \times \left\{ 1 + \sqrt{1 + \frac{2E}{9\rho_s (1 - \nu) Q} \left[\frac{(3f_p - 1)\gamma + (1 - f_p)}{f_p (\gamma - 1)(3\gamma - 1)} \right]^2} \right\} \tag{15}$$

where $Q = Y/m$, the energy density. Thus, μ is a function of the deposited energy yield, the mass impacting the vessel wall, and γ of the contained propellant-vapor mixture. However, γ is also a function of the energy density Q, and the mass density ρ of the contained vapor/propellant gas, $\gamma(\rho, Q)$.

For a fixed Δh, R is given by

$$R = \sqrt{\frac{\mu Y}{4\pi \rho_s \Delta h}} \tag{16}$$

yielding the following propellant-vapor gas density:

$$\rho = 6\sqrt{\pi} m \left(\frac{\rho_s \Delta h}{\mu Y} \right)^{3/2} \tag{17}$$

Equations (15) and (17) imply that for a fixed yield, γ is a function of the mass impacting the wall and μ. No explicit relation for μ can be found.

The mass of the contained propellant-vapor gas is made up of m_d, m_0, and m_v:

$$m = m_d + m_0 + m_v \tag{18}$$

The γ for the propellant-vapor mixture is a mass weighted value:

$$\gamma = \frac{\gamma_d m_d + \gamma_0 m_0 + \gamma_v m_v}{m_d + m_0 + m_v} \tag{19}$$

If the mass of the device and of the vaporized liner are small compared to the propellant mass then, from Eqs. (17) and (18), $m \approx m_0$, $\rho \approx \rho_0$, and $\gamma(\rho_0, m_0)$ for a fixed yield. Equations (15) and (17) are rewritten as

$$\mu = \frac{3[\gamma(\rho_0, m_0) - 1]\rho_s}{2\sigma_{max}} \left(1 + \sqrt{1 + \frac{2Em_0}{9\rho_s (1 - \nu) Y} \left\{ \frac{(3f_p - 1)\gamma(\rho_0, m_0) + (1 - f_p)}{f_p [\gamma(\rho_0, m_0) - 1][3\gamma(\rho_0, m_0) - 1]} \right\}^2} \right) \tag{20}$$

$$\rho = 6\sqrt{\pi} m_0 \left(\frac{\rho_s \Delta h}{\mu Y} \right)^{3/2} \tag{21}$$

For a given yield and a given propellant gas mass, Eqs. (20) and (21) are solved iteratively to obtain the parameter μ for a monolithic, spherical vessel.

Thrust and Specific Impulse Evaluation Theory

In order to evaluate the propulsive performance of the CPNP concept, it is necessary to obtain expressions for the evaluation of the unsteady propellant mass flow rate at the nozzle throat, and the propellant exhaust velocity at the exit of the supersonic nozzle. Then, the engine thrust and specific impulse can be calculated, along with the engine thrust to weight ratio.

The initial vessel pressure, immediately following the detonation, can be calculated from a modified form of the gamma-gas law, Eq. (9)

$$p_{cont}(t = 0) = p_0 = (\gamma - 1) \frac{(Y - H_l m_v)}{V_{vessel}} \tag{22}$$

Equation (22) is slightly different than Eq. (9) in that it accounts for the amount of energy necessary to vaporize the liner. The critical pressure in the containment vessel is the pressure that establishes sonic flow at the nozzle throat. Assuming isentropic flow of the propellant-vapor through the nozzle[12]:

$$\frac{p_{cont}(t)}{p_{ambient}} \geq \left[\frac{\gamma + 1}{2} \right]^{\gamma/\gamma - 1} \tag{23}$$

In Eq. (23) the equal sign applies to a sonic nozzle, and the greater than sign applies to a supersonic nozzle. The pressure and temperature transients of the propellant-vapor mixture in the vessel are calculated using

$$p_{cont}(t) = p_{cont}(t = 0) \left[\frac{\rho_{cont}(t)}{\rho_{cont}(t = 0)} \right]^{\gamma} \tag{24}$$

$$T_{cont}(t) = T_{cont}(t = 0) \left[\frac{\rho_{cont}(t)}{\rho_{cont}(t = 0)} \right]^{\gamma - 1} \tag{25}$$

where the initial values of the contained propellant-vapor mixture temperature and pressure are the values of the tem-

perature and pressure in the containment vessel immediately following the detonation.

For values of the containment vessel pressure larger than the critical pressure, the propellant-vapor mixture discharge rate, the maximum flow rate, through a sonic nozzle is given by[12]

$$\dot{m}(t)_{\text{sonic}} = S_N \sqrt{\gamma P_{\text{cont}}(t)\rho_{\text{cont}}(t)\left(\frac{2}{\gamma+1}\right)^{(\gamma+1)/(\gamma-1)}} \tag{26}$$

where S_N is the area of the nozzle throat. The discharge time required to reduce the density of the propellant-vapor mixture in the vessel to $\rho_{\text{cont}}(t)$ is[12]

$$t_{\text{exh}} = \frac{V_{\text{vessel}}}{S_N \sqrt{\gamma\left[\frac{p_{\text{cont}}(0)}{\rho_{\text{cont}}(0)}\right]\left(\frac{2}{\gamma+1}\right)^{(\gamma+1)/(\gamma-1)}}} \times \left(\frac{2}{\gamma-1}\right)\left\{\left[\frac{\rho_{\text{cont}}(t)}{\rho_{\text{cont}}(t=0)}\right]^{(1-\gamma)/2} - 1\right\} \tag{27}$$

Once the pressure in the containment vessel is less than the critical pressure, the mass flow rate of the propellant-vapor mixture discharge is

$$\dot{m}(t) = S_N \sqrt{p_{\text{cont}}(t)\rho_{\text{cont}}(t)\left(\frac{2\gamma}{\gamma-1}\right)\left\{\left[\frac{p_{\text{ambient}}}{p_{\text{cont}}(t)}\right]^{(2/\gamma)} - \left[\frac{p_{\text{ambient}}}{p_{\text{cont}}(t)}\right]^{(\gamma+1)/\gamma}\right\}} \tag{28}$$

and the discharge time for a specified density is

$$t_{\text{exh}} = \frac{V_{\text{vessel}}}{S_N \sqrt{\frac{p_{\text{cont}}}{\rho_{\text{cont}}(t=0)}\left(\frac{2\gamma}{\gamma+1}\right)}} \int_{\rho_{\text{cont}}(t)/\rho_{\text{cont}}(0)}^{1} \frac{d\eta}{\sqrt{\left[\frac{p_{\text{ambient}}}{p_{\text{cont}}(0)}\right]^{2/\gamma}\eta^{\gamma-1} - \left[\frac{p_{\text{ambient}}}{P_{\text{cont}}(0)}\right]^{(\gamma+1)/\gamma}}} \tag{29}$$

For a diverging (supersonic) nozzle, the propellant-vapor mixture's theoretical maximum exhaust velocity is calculated quasistatically using[13]

$$V_e(t) = \sqrt{\frac{2\gamma}{\gamma-1}RT_{\text{cont}}(t)} \tag{30}$$

where R is the mass-averaged propellant-vapor mixture gas constant. Equation (30) is based upon expanding the propellant to a vacuum. The corresponding engine thrust is calculated from

$$F_N(t) = \dot{m}(t)V_e(t) \tag{31}$$

and the corresponding engine specific impulse is evaluated by

$$I_{\text{sp}}(t) = (V_e(t)/g) \tag{32}$$

The engine thrust-to-weight ratio is calculated by dividing Eq. (31) by Eq. (10).

Material Considerations

One of the main conclusions of the HELIOS and of the ORION studies was that both concepts were hindered by the unavailability of materials strong enough to tolerate the cyclic dynamic loads experienced following nuclear detonations.[3,7] In the 25–30 yr since the HELIOS and ORION studies, materials technology has made significant breakthroughs. This study has investigated alternative materials for use in the vessel and the liner.

In investigating a variety of structural materials for the containment vessel, an effort was made to consider the significant recent advances in the field of high-strength, high-temperature composite materials. Currently, there are a number of manufacturers providing SiC-based composite fibers, also known as SYLRAMICS, which can be woven into a metal matrix.[14,15] One such material is NICALON™.[15]

NICALON SiC fiber is a continuous fiber manufactured by an exclusive polymer pyrolysis process. NICALON is composed of ultrafine β-SiC crystals exhibiting a tensile strength of over 2.41×10^9 Pa (350,000 psi) and a tensile modulus (Young's modulus) over 1.72×10^{11} Pa (25,000,000 psi). The fiber is 10–15 μ in diameter, and it retains its physical properties at temperatures in excess of 1400 K. Furthermore, NICALON fiber is an excellent choice as a reinforcement for metal matrix composites. The fiber is readily wet in metals, and it can be woven into cloth and preformed shapes. This allows composite design and manufacturing for a variety of applications. The large specific strength and Young's modulus of the NICALON fibers, and their retention of these properties at high temperatures, results in metal composites with improved mechanical properties. Additionally, flexural fatigue tests have shown that NICALON metal matrix composites retain a significant portion of their strength following up to 10^7 cycles.[15] Table 1 compares the strength of various stainless steels considered for use in this analysis.

A NICALON fiber reinforced stainless steel is chosen as the containment vessel material for this study. The composite material is assumed to have a yield tensile strength of 1.57×10^9 Pa (160 kgf/mm^2), less than 50% of the maximum value in Table 1. This assumption is based upon two considerations. First, the vessel will experience less than 500,000 cycles, or 5% of the 10^7 cycles quoted. Second, the dynamic response investigated using CHARTD was for a closed vessel and not a vented vessel. As a result of the low volume fraction of the fibers in the metal matrix, the effective density of the composite material is assumed to be that of stainless steel. Since Young's modulus for the NICALON fiber is similar to that for stainless steel, Young's modulus and the Poisson ratio for the composite is assumed to be the same as for a standard stainless steel: $E = 2 \times 10^{11}$ Pa, $\nu = 0.29$.

Table 1 Comparison of yield tensile strength of stainless steels and stainless steel composites

Material	Yield tensile strength,[a] Pa	Yield tensile strength, kgf/mm^2
SS 304	5.49×10^8	56.0
SS 304L	4.80×10^8	49.0
SS 316	5.15×10^8	52.5
SS 316L	4.80×10^8	49.0
SS 347	5.15×10^8	52.5
High-strength steel	6.9×10^8	70.4
SS w/Nextel™ 312 fibers[14]	1.69×10^9	172.0
SS w/NICALON SiC fibers[15]	2.45×10^9–3.24×10^9	250.0–330.0

[a]0.2% offset.

Parametric Studies Using the CHARTD Hydrodynamic Code

In designing the vessel for the CPNP system, it becomes necessary to optimize a number of variables which are interrelated and contribute towards the overall mass of the containment vessel. For example, it is necessary to find the optimal yield value, because even though lower values of the yield will result in less massive vessels, they will generally require more detonations to achieve the desired ΔV for a given mission. This in turn will require the design of a containment vessel which is more fatigue resistant. Additional parameters, such as the initial pressure of the propellant gas in the vessel and the time intervals of the detonations, must be determined through extensive parametric studies. The geometry of the vessel can also be subject to optimization, improving the overall containment vessel design.

The study by Davidson et al.[9] used the one-dimensional, Lagrangian, radiation-coupled hydrodynamic computer code CHARTD[10] to investigate the containment of a nuclear detonation in a monolithic, unvented, spherical steel containment vessel with an ablation liner. The study assumed that the vessel is initially filled with air and parametrically investigated the effect of the initial air pressure, the liner material, and the thickness of the liner material on the mechanical response of the vessel. As its baseline, the study used a 100-ton (4.2×10^{11} J) nuclear device. The aluminum liner was assumed to be 0.01-m thick with a snug fit against the containment vessel. The initial air pressure in the containment vessel for the study was 50 Torr (1 Torr = 133.32 Pa). The results of calculations using the analytical model presented in the previous section suggests a 0.20-m-thick vessel with an outer radius of 14.34 m.

Initial Gas Pressure

The parametric study varied the initial air pressure from 1 Torr to 1 atm (1 atm = 760 Torr = 101,325 Pa) while using the baseline vessel parameters. The resulting hoop stresses induced in the containment vessel are compared to the yield stress of the steel, 6.9×10^8 Pa: in each case the radial stress was less than the hoop stress. The parametric studies indicated that the hoop stress is a minimum for an initial air pressure of 50 Torr: for an initial air pressure of 1 Torr the hoop stress in the containment vessel is 6.1×10^8 Pa, 5.0×10^8 Pa for 50 Torr, and 8.4×10^8 Pa for 1 atm, exceeding the 6.9×10^8 Pa yield stress of high-strength steel. Also, the amount of liner vaporized during the initial few milliseconds decreased with increasing initial air pressure. The analysis also indicated that a low initial air pressure resulted in more frequent shock waves: initially the shock waves have a larger amplitude, but they damp out quickly.

The CHARTD parametric results were also used to verify the validity of the scaling relations for μ and ρ presented in Eqs. (20) and (21).[9] To solve Eqs. (20) and (21) iteratively requires $\gamma(\rho_0, m_0)$. For this study the equation-of-state tables with CHARTD were used. Comparing the value of μ determined by Eqs. (20) and (21) to the CHARTD results indicates that 1) μ increases linearly with the initial pressure (mass) of the air in the vessel except at low initial pressures, and 2) that the scaling law is valid except at low initial air pressure (mass) in the vessel. For the base case described, the μ determined by the scaling law are valid for initial air pressures of 50 Torr and above. The μ scaled linearly from 30 at an initial air pressure of 50 Torr to 50 for an initial pressure of 500 Torr.[9] For conservatism, the baseline μ for this study was chosen to be 40 tonnes of vessel mass per ton of nuclear yield.

The reason that μ does not scale with the initial air pressure and that the scaling law is not valid at low initial air pressures is due to the effect of the liner vapor. As implied above, at low initial air pressures the amount of liner vaporized increased. When the mass of the liner vapor is of the same order then the mass of the air in the vessel, μ becomes a function of the air mass and the vapor mass; also, the scaling relation is not valid because it assumed that the air mass is much greater than the liner vapor mass and the device mass.

Liner Material

As stated, the parametric study considered the effect of various liner materials: aluminum, tungsten, lead, and molybdenum. The materials were chosen to cover a range of vaporization temperatures, and combined latent heat of vaporization and sensible energy required to raise the temperature of the material to vapor temperatures. The CHARTD results are supported by an analytical solution to the transient, heat-conduction equation, using an integral heat balance approach, for the ablation of a semi-infinite slab.[9,16] The CHARTD results indicate that of the four materials considered, tungsten and molybdenum are the liner materials that provide the best protection for the containment vessel; i.e., the lowest peak hoop stress. Lead was the worst material for the liner, resulting in the largest peak hoop stress. Aluminum fell in between the two extremes.[9] Young's modulus for molybdenum and tungsten are significantly higher than for steel, while lead and aluminum have a smaller Young's modulus than steel. Although the liner is thin in comparison to the steel vessel, its strength can provide some protection for the steel vessel. In each of the cases, the radial stress was less than the hoop stress.

The CHARTD studies indicate that the molybdenum liner lost less mass due to ablation than the other materials. Both molybdenum and aluminum lost less mass on the initial shock: these materials require a large amount of energy per unit mass to go from room temperature to a vapor when compared to lead and tungsten. Molybdenum and tungsten lost most of their mass on the initial shock and very little on subsequent shocks. Aluminum and lead continued to ablate on subsequent shocks.

The analytical study provided insight into the reason that the molybdenum and tungsten liners did not have much additional ablation after the first shock.[9] Both molybdenum and tungsten required a longer time to reach a steady-state ablation rate, and at steady state had longer characteristic lengths for the ablation and thermal depths. The thermal depth is the length that the temperature distribution penetrates the semi-infinite slab, and the ablation depth is the thickness of the ablation layer. Shock heating is short-time duration, unsteady heating. The secondary shocks are small enough, even in an unvented vessel, that substantial ablation of the molybdenum and tungsten liners does not occur: in a vented vessel the secondary shocks would be less.

The combination of material properties that provide an indication of a material's ability to resist deterioration from the shocks in the vessel comes from the analytical solution to the transient heat conduction equation for the ablation of a semi-infinite slab using the integral heat balance approach:

$$\nu_{\text{ablation}} = \frac{\alpha_l H_l \rho_l}{k_l T_l} \tag{33}$$

In Eq. (33) the larger the value of ν_{ablation} is, the more resistant the material is to ablation from the shock waves. Table 2 provides a summary of the materials study results, along with representative material properties. As can be observed, both molybdenum and tungsten have larger ν_{ablation} than lead and aluminum.

The characteristics of the liner material should include a high Young's modulus, a large heat of vaporization, and large ν_{ablation}. Taking into account both the protection it provides to the containment vessel and its ability to resist ablative mass loss, the largest value of ν_{ablation}, molybdenum is the best overall material of the four considered.

Table 2 Comparison of liner materials

	Aluminum	Molybdenum	Tungsten	Lead
Material properties				
Density, kg/m^3	2,700	10,220	19,300	11,350
Heat to vaporization (from 300 K), J/kg	1.57×10^7	1.58×10^7	5.67×10^6	1.20×10^6
Thermal conductivity, W/m-K	213 @ 900 K	88 @ 2,000 K	100 @ 2,000 K	31.2 @ 600 K
Thermal diffusivity, m^2/s	9.05×10^{-5}	3.74×10^{-5}	4.68×10^{-5}	2.17×10^{-5}
ν_{ablation} (T_i = 300 K)	58.1	201.3	113.8	29.8
Young's modulus, Pa	6.89×10^{10}	2.76×10^{11}	3.45×10^{11}	1.38×10^{10}
CHARTD Results				
Maximum hoop stress, Pa	5.1×10^8	4.35×10^8	4.3×10^8	5.7×10^8
Mass of liner vapor at 2 ms/7 ms, kg	210/960	590/590	1,700/1,700	13,000/27,000
Analytical results (steady-state values)				
Ablation time, s	0.00113	0.00298	0.00387	1.84×10^{-5}
Ablation layer, m	0.00067	0.00071	0.00091	0.000042
Thermal layer, m	0.00128	0.00134	0.00170	0.00008

Liner Thickness

Based upon the baseline case, CHARTD was used to examine the tradeoff between a 0.01-m- vs a 0.05-m-thick aluminum liner. The results from CHARTD showed that the 0.05-m-thick aluminum liner provided more protection for the steel vessel than the 0.01-m liner; i.e., the thicker liner provided approximately a 4% lower maximum hoop stress for a factor of 5 increase in the liner thickness. The increase in the liner thickness is expected to exhibit a similar trend in the results for other liner materials.

CPNP Performance Analysis Results

In this section the pressure vessel scaling, the equations for the thrust and specific impulse, the material considerations, and the results of the hydrodynamic parametric study are applied to analyze the performance of a CPNP engine. For this study a 100-ton nuclear device is assumed. This yield is chosen for the study because of the supporting analysis by Davidson et al.[9] For an in-depth conceptual design study, a parametric analysis of the yield would need to be undertaken, considering the mission. For the purposes of this preliminary analysis, a number of the parameters have been also set in accordance with the study by Davidson et al.[9] Because this referenced study did not pertain to propulsive uses, it is believed that further refinements of these parameters will improve the concept performance.

A summary of the parameters used in this analysis is given in Table 3. As can be seen, the differences from the parametric study in the previous section are that the liner is molybdenum; the properties of the liner are set accordingly (Table 2). The other difference is that the propellant is hydrogen, not air. The vessel is charged with hydrogen at a density equal to the density of air in the parameter study described in the previous section. Based upon the ideal gas law, the density of 50 Torr of air is equal to the density of 720 Torr of hydrogen, due to the difference in their molecular weights.

For a 100-ton nuclear device, and with the other parameters as in Table 3, Eqs. (20), and (21) are solved iteratively to determine the μ and the radius of the containment vessel. Since the parameters in Table 3 are set to be similar to the cases discussed in the hydrodynamic parametric study, a μ of 40 MT/ton of yield is chosen for this analysis. This value of μ includes a 25% margin. As stated above, this value of μ is for high-strength stainless-steel. The value of μ, Eq. (20), scales inversely with the yield strength of the material; thus, for stainless steel reinforced with NICALON fibers, μ is 17.5 MT/ton of yield. The high-strength stainless vessel has a radius of 14.23 m and a mass of 4000 MT. The vessel made of the stainless steel reinforced with NICALON fibers has a radius of 9.4 m and a mass of 1750 MT. To account for fatigue the ultimate strength of the composite stainless steel chosen for the analysis is 1.57×10^9 Pa, whereas the ultimate strength of the high-strength stainless steel is 6.9×10^8 Pa. As stated in the section on materials, the Young's modulus, Poisson ratio, and the density for the composite stainless steel is assumed to be the same as for the stainless steel.

Table 3 Input parameters for CPNP performance analysis

Parameter	Input value
f_p, Eq. (14)	0.25
Yield	100 tons (4.184×10^{11} J)
Containment vessel wall thickness	0.20 m
Containment vessel material density	7.86×10^3 kg/m^3
Initial ambient pressure	50 Torr (6,552 Pa)
Liner material	Molybdenum
Liner thickness	0.01 m
Liner vapor mass	590 kg[a]
Liner vapor density	4.89×10^{-2} kg/m^3
Liner γ	1.4
Liner vapor gas constant	8.71×10^1 J/(kg-K)
Propellant	Hydrogen
Propellant specific heat	6.45×10^3 J/(kg-K)
Propellant γ	1.2675
Propellant gas constant	4.12×10^3 J/(kg-K)
Propellant initial pressure	720 Torr (95,904 Pa)
Propellant initial density	7.76×10^{-2} kg/m^3
Propellant initial temperature	300 K
Propellant temperature following detonation	5 eV (24,205 K)[a]

[a]Input value from CHARTD results for an equal mass of air under similar conditions.[9]

The stronger composite material also results in a smaller propellant mass per shot, assuming equal initial propellant densities: 936 kg of hydrogen per shot for the 14.23-m vs 271 kg for the 9.41-m vessel. The stronger composite material allows for a more efficient propulsive shot since the same amount of energy is deposited into a smaller mass of propellant. This estimate of the propellant mass, and all other estimates below, are very dependent upon the size of the device. For example, based upon the composite material, and all other parameters held constant, a 20-ton device would require a 4.2-m vessel, having a mass of 350 MT, and requiring 2.4 kg of propellant.

Table 3 lists the amount of molybdenum liner ablated per shot as 590 kg. This value corresponds to the amount of liner

ablated for the 14.23-m vessel filled with air at 50 Torr. The study by Davidson et al.[9] did not characterize the amount of liner ablated as a function of the vessel's radius (surface area) or the molecular weight of the fill gas. Assuming 590 kg of molybdenum ablated is conservative in determining the thrust associated with a shot, since it results in a high, effective molecular weight of the propellant. The section "Thrust and Specific Impulse Evaluation Theory" incorporated the effect of the liner vapor into the equations for the thrust and the specific impulse, Eqs. (30–32). In contrast, the high vapor mass makes the calculation and scaling determination of the radius and μ of the vessel using Eqs. (16), (20), and (21) not conservative. However, as stated in the subsection "Initial Gas Pressure" the 40 tonnes per ton is a 25% increase over the 30 tonnes per ton indicated by the hydrodynamic study and the scaling relation. From the scaling relationship Davidson et al.[9] showed that for a fixed radius vessel, 14.23 m, and a 100-ton device, the 40 tonnes per ton is adequate for up to 5000 kg of fill gas. The combined mass of the hydrogen, 271 kg, and the liner vapor, 590 kg, is less than 1000 kg. For this concept analysis, the parameters assumed appear to result in a conservative estimate of the vessel radius and μ; however, the uncertainty indicates an area requiring further study.

The pressure and temperature transients in the vessel following the detonations are based upon the vessel having a supersonic nozzle with a throat radius that is 10 and 20% of the vessel radius. Based on these nozzle specifications, the chamber pressure and temperature transients are calculated using Eqs. (24) and (25). These transients are shown in Figs. 2 and 3. The rate at which the impulse decays away is dependent upon the throat radius. For throat radii that are 10 and 20% of the vessel radius, the pressure in the chamber drops below the critical pressure in approximately 0.8 s and 0.2 s, respectively. The temperature of the propellant in the chamber drops to approximately 3000 K in these time spans. In the latter case the chamber temperature drops to 2000 K in approximately 0.3 s, but in the former it takes longer than 1 s. These results indicate the necessity in a more detailed study for a thermal analysis of the vessel.

The propellant mass flow rate is determined from Eqs. (26–29), the propellant exhaust velocity is evaluated from Eq. (30), and the engine thrust is calculated using Eq. (31). The exit velocity and thrust is based upon an infinite expansion ratio, the theoretical maximum. As a point of reference, an expansion area ratio of 77.5, corresponding to the Space Shuttle Main Engine (SSME) nozzle specifications, results in a nozzle exit radius of approximately the size of the vessel radius.[13] The resulting engine thrust transient is depicted in Fig. 4. The average thrust is estimated to be approximately 5.0×10^6 N for the vessel with a throat radius of 10% of the vessel radius and 2.0×10^7 N for the vessel with a throat radius of 20% of the vessel radius. The maximum thrust in each case is 4.6×10^7 and 1.9×10^8 N, respectively. The thrust-to-weight ratio is calculated and shown in Fig. 5. The vessel

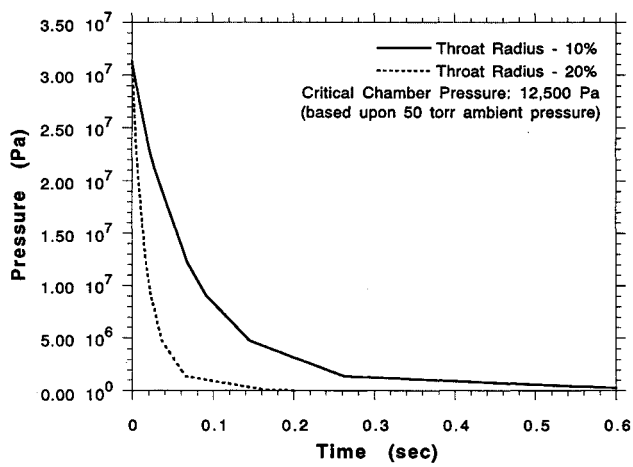

Fig. 2 Pressure transient in a 9.4-m containment vessel charged with hydrogen at 720 Torr after the detonation of a 100-ton yield nuclear device.

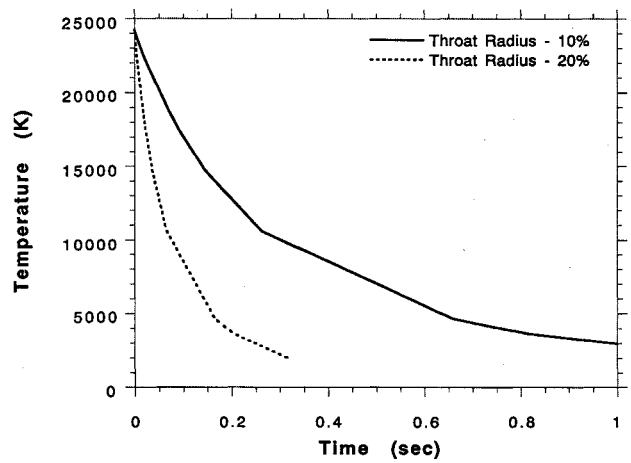

Fig. 3 Temperature transient in a 9.4-m containment vessel charged with hydrogen at 720 Torr after the detonation of a 100-ton yield nuclear device.

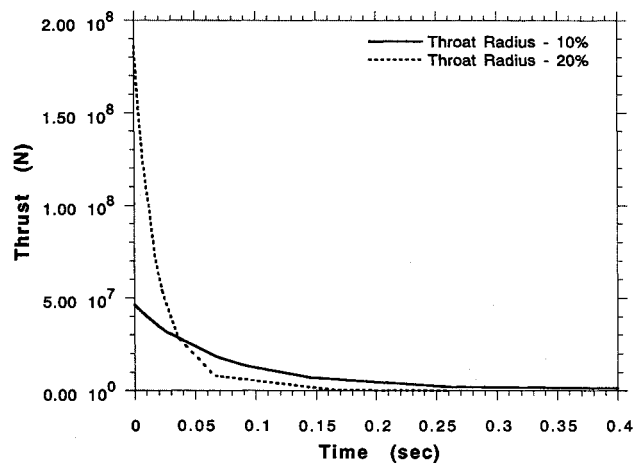

Fig. 4 Thrust, as a function of time, from a supersonic nozzle after the detonation of a 100-ton yield nuclear device in a 9.4-m containment vessel initially charged with hydrogen at 720 Torr.

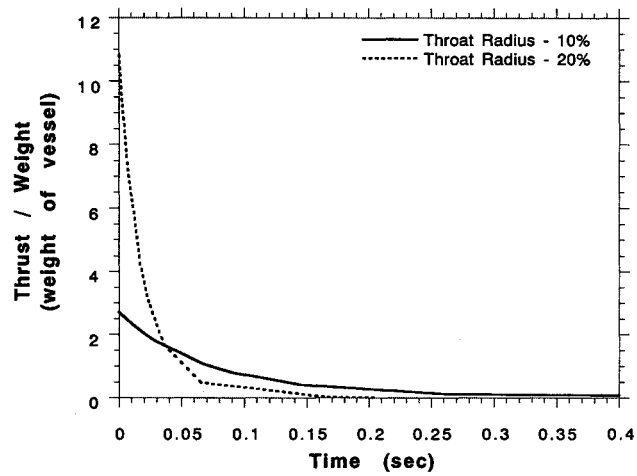

Fig. 5 Thrust-to-weight ratio, as a function of time, of a CPNP engine. Based upon a 1750-MT vessel and the detonation of a 100-ton yield nuclear device in a 9.4-m containment vessel initially charged with hydrogen at 720 Torr.

weight is 1.7×10^7 N. The average thrust-to-weight ratio during the vessel blowdown is 0.28 for the small throat and 1.1 for the larger throat.

Figure 6 plots the resulting specific impulse during the engine operation. As shown in Fig. 6, the specific impulse of a CPNP engine varies from a high of 1600 s at the beginning of the pulse to 600 s at the end of a pulse, with an average specific impulse of 980 s.

For a point of reference, the performance parameters of the CPNP just presented are compared to a gas-core rocket engine. A presentation given at a recent workshop on gas-core nuclear rockets gave a range of thrusts of 22–440 kN for a 5000-s burn. The thrust-to-weight ratio for gas-core concepts are between 0.1–0.7. The specific impulse of a gas core engine is in the range of 4000–6000 s, and is limited by the cooling requirements of the containment vessel wall and nozzle.[1]

The size of the nozzle's throat determines the length of the effective thrust, the maximum thrust, and the average thrust per shot. However, the mass of the propellant and the energy of the device is the same, and thus, the integrated thrust and the average specific impulse is the same regardless of the throat size. Just as for a steady-state chemical or nuclear rocket, the performance of the CPNP engine is dependent upon the molecular weight of the propellant and the temperature of the propellant.

To determine the number of detonations required for a mission, the ΔV requirement of the mission needs to be specified. The increase in velocity of a spacecraft powered by a CPNP engine can be estimated using a simple impulse-momentum balance, based upon an average thrust per shot

$$\Delta V = \frac{nF_N(\text{ave})t_{\text{exh}}}{M_{\text{veh}}} \tag{34}$$

where n is the number of shots, $F_N(\text{ave})$ is the average thrust per shot, Eq. (31), and t_{exh} is the duration of the blowdown of the vessel, Eqs. (27) and (29). M_{veh} is the mass of the containment vessel, Eq. (10), the mass of the payload, and the mass of associated CPNP components such as the propellant and its tanks, the devices, shielding for the devices and payload, and the supporting structure.

For example, the integrated thrust, $F_N(\text{ave}) \times t_{\text{exh}}$, of a 100-ton yield is 4.0×10^6 N-s. To increase the velocity of the vehicle by 1 kg/s per 1000 metric tonnes of vehicle mass would require approximately 250 100-ton nuclear shots. In general, the total ΔV necessary for a mission to the Moon or Mars from LEO is 4.5 km/s; approximately 3 km/s to escape Earth, and 1–1.5 km/s to enter orbit around the Moon or Mars.

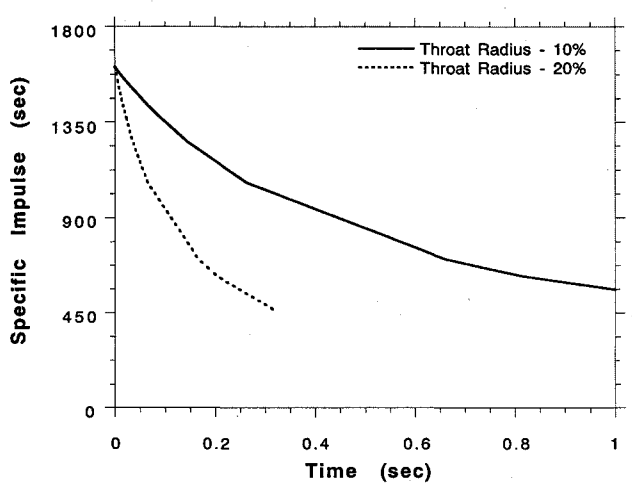

Fig. 6 Specific impulse, as a function of time, of a CPNP engine. Based upon a 1750-MT vessel and the detonation of a 100-ton yield nuclear device in a 9.4-m containment vessel initially charged with hydrogen at 720 Torr.

Assuming a total vehicle mass of 4000 MT, the number of shots required would be less than 5000. As stated above, the composite stainless steel retains significant strength up to 10^7 cycles.

Assuming that 590 kg of the molybdenum liner is vaporized and lost on every shot, the liner has a lifetime of 190 shots. In light of the numbers given in the previous paragraph, this in not adequate. However, there are three factors to be considered:

1) Increasing the initial propellant mass reduces the mass of the liner vaporized, increases the integrated thrust, reduces the number of required detonations, but also increases the hoop stress in the vessel.

2) Increasing the liner thickness increases its lifetime, but also increases the vessel's mass.

3) Since the amount of liner vaporized is based upon a closed vessel analysis, a vented vessel may result in a smaller liner mass vaporized. This indicates that a viable CPNP concept requires a tradeoff between the life of the liner, the induced fatigue of the vessel, and the mass of the vessel. It also requires a hydrodynamic characterization of the effect of a vented vessel, the propellant, and the vessel radius on the liner lifetime.

Conclusions

This article presents the results of a scoping study that assessed the viability of using contained nuclear detonations as a means of impulsive space nuclear propulsion. The obvious motivation for this type of concept is the high-energy density of a nuclear device and the subsequent high velocity that it can impart to a propellant. In the 1950s and 1960s a CPNP concept was investigated under the program name HELIOS. The results of this study indicated that the concept had potential, but the material technology was not at a mature enough stage to support its further development at the time. Presently, the concept's potential still exists and the material technology has developed to a stage to warrant further study. This article presents the results of the initial contemporary scoping study for a CPNP concept.

Presented is the approach for the scaling of a containment vessel and the macroscopic energy and mass balance analysis for the discharge of the propellant. A summary is provided of the material properties of composite stainless steel that is reinforced with SiC fiber. The literature shows that the composite stainless steel has an ultimate strength that is 4–6 times greater than standard stainless steel or high-strength steels. This increase in material strength translates directly into a reduction in the size of the containment vessel, the mass of the containment vessel, and the number of shots needed to attain a desired ΔV. The composite material also retains substantial strength after a large number of cycles. The results of a hydrodynamic parametric study also provide guidance on the effect of the initial propellant pressure on the response of the containment vessel. This parametric study also indicates that the choice of a liner material has an impact on the vessel response and on the longevity of the vessel.

Based on the vessel scaling and material studies, this article presents a scoping analysis that indicates that the CPNP engine is a viable concept, but requires further study to identify the design parameters that will result in the optimum concept performance. In the context of advanced propulsion concepts being studied at this time, the CPNP concept is most closely related to the open-cycle, gas-core nuclear engine. The apparent parallels are that they are open-ended nuclear concepts and that both appear to have attractive attributes, such as very high propellant temperatures.

Both concepts need to consider shielding for the payloads. The shielding, however, are different problems. The CPNP shielding problem is characterized by a number of bursts of fission neutrons and gammas. The shielding for residual radiation is primarily for activation of the vessel and adjacent

structures; however, due to the nature of the fast fission chain reaction there should be very few long-life fission products produced. The gas-core is essentially a steady-state reactor. The shielding would be from the neutrons and gammas produced in the gas-core engine at a lower flux than the CPNP, but probably for a longer duration. The residual radiation would need to consider an inventory of long-life fission products.

According to a presentation in Ref. 1, the implementation of a gas-core engine is dependent on the development of turbopump assemblies that can meet the design requirements of the gas-core reactor. While the CPNP does not require high-duty cycle turbopump assemblies, it must meet the design challenge of the storage, injection, and detonation of a large number of small nuclear devices. However, the gas-core concepts present a number of additional very difficult physics and engineering challenges; e.g., plasma confinement, startup, both hydrodynamic and nuclear stability, material considerations at flow boundaries, and nozzle design.[1] In contrast, the CPNP engine is basically a simplistic design based upon current technology.

After a complete study to identify the best overall design, it is conceivable that a CPNP engine could be built and tested without similar physics and engineering challenges. The hydrodynamics, vessel response, blowdown, and thermal aspects of the basic concept can be tested and evaluated via nonnuclear means using high-energy explosives. A potential application is as a workhorse, cargo transport for large loads to the Moon and Mars. Because of its simplicity there is no reason to believe that it would not be a relatively cheap rocket engine to build and operate.

As indicated from the scoping analysis for a CPNP engine, a number of trade studies must be made and problems addressed. A complete design study would have to include comprehensive research of the work that was done on the HELIOS concept in the 1950s and 1960s to ascertain the extent of the analysis. The study will need to utilize the advances in materials, computational methods, and capabilities over the past 25–30 yr since the concept was last investigated. This would include the application of state-of-the-art hydrodynamic, computational fluid dynamics, thermal, and structural models to define a working concept design. A conceptual design study would have to address the engineering design aspects of the concept: nuclear device design, injection of the nuclear device, injection of the propellant, shielding and storage of the nuclear devices, etc. Finally, a complete study will need to include mission analysis to identify the class of missions that will benefit from a CPNP engine.

Acknowledgments

We acknowledge J. W. Davidson and A. R. Larson of Los Alamos National Laboratory, New Mexico, for their contribution in Ref. 9 that is applied to this study; i.e., the derivation of the scaling relation presented in the section "Pressure Vessel Scaling."

References

[1]Borowski, S. K., "The LeRC Open Cycle Gas Core Rocket Program," *Proceedings of the Gas Core Nuclear Rocket Workshop*," Los Alamos National Lab., LA-UR-91-1250, Boulder, CO, April 1991.

[2]Howe, S. D., Borowski, S., Motloch, C., Helms, I., Diaz, N., Anghaie, S., and Latham, T., "Innovative Nuclear Thermal Propulsion Technology Evaluation: Results of the NASA/DOE Task Team Study," 42nd Congress of the International Astronautical Fed., Paper IAF-91-235, Montreal, Canada, Oct. 1991.

[3]Nance, J. C., "Nuclear Pulse Propulsion," *IEEE Transactions on Nuclear Science*, Vol. NS-12, No. 1, 1965, pp. 177–182.

[4]Augenstein, B. W., "Some Aspects of Interstellar Space Exploration—New Orion Systems, Early Precursor Missions," 42nd Congress of the International Astronautical Fed., Paper IAF-91-716, Montreal, Canada, Oct. 1991.

[5]Cole, D. M., "The Feasibility of Propelling Vehicles by Contained Nuclear Explosions," 6th National Annual Meeting, American Astronautical Society, The Martin Co., NY, Jan. 1960.

[6]Fox, R. H., "A Study of the Nuclear Gaseous Reactor Rocket," Lawrence Radiation Lab., Rept. UCRL-4996, Livermore, CA, 1957.

[7]Hadley, J. W., Stubbs, T. F., Janssen, M. A., and Simons, L. A., "The Helios Pulsed Nuclear Propulsion Concept," Lawrence Radiation Lab., Rept. UCRL-14238, Livermore, CA, June 1965.

[8]Eidelman, S., Grossmann, W., and Lottati, I., "Review of Propulsion Applications and Numerical Simulations of the Pulsed Detonation Engine Concept," *Journal of Propulsion and Power*, Vol. 7, No. 6, 1991, pp. 857–865.

[9]Davidson, J. W., Larson, A. R., Metzger, J. D., Keller, C. E., Lowry, W. E., Mattingly, P., Ruiz, N. K., and Walsh, R. T., "Containment of the Blast and Thermal Energy of a Nuclear Explosive in a Monolithic, Spherical Steel Vessel with a Metal Liner," Draft Los Alamos National Lab. Rept. (unclassified draft report), Los Alamos, NM, Oct. 1988.

[10]Thompson, S. L., and Lauson, H. S., "Improvements in the CHARTD Radiation-Hydrodynamics Code III: Revised Analytical Equation of State," Sandia National Lab. Rept. SC-RR-71-0714, Albuquerque, NM, March 1972.

[11]Zel'dovich, Y. B., and Raizer, Y. P., *Physics of Shock Waves and High-Temperature Hydrodynamic Phenomena*, Vol. 1, Academic Press, New York, 1966, Chap. IV.

[12]Bird, R. B., Stewart, W. E., and Lightfoot, E. N., *Transport Phenomena*, Wiley, New York, 1960, Chap. 15.

[13]Sutton, G. P., *Rocket Propulsion Elements, An Introduction to the Engineering of Rockets*, 5th ed., Wiley, New York, 1986, Chaps. 3 and 9.

[14]"Nextel℠ Ceramic Fiber Products for High Temperature Applications," New Product Information, The 3M Corp., St. Paul, MN, Jan. 1984.

[15]"SYLRAMICS—The Technology of Silicon Ceramics," New Product Information, Dow Corning Corp., Midland, MI, 1985.

[16]Özisik, M. N., *Boundary Value Problems in Heat Conduction*, International Textbook Co., Scranton, PA, 1968, Chap. 7.